COMPDYN 2021
8th ECCOMAS Thematic Conference on
Computational Methods in Structural Dynamics and Earthquake Engineering
M. Papadrakakis, M. Fragiadakis (eds.)
Streamed from Athens, Greece, 27–30 June 2021

INNOVATIVE MASS-DAMPING-BASED APPROACHES FOR SEISMIC DESIGN OF TALL BUILDINGS

Elena Mele[1,*], Diana Faiella[2], and Mario Argenziano[3]

[1,*] University of Naples Federico II
Dept. Structures for Engineering and Architecture
P.le Tecchio 80
elenmele@unina.it (corresponding author)

[2] University of Naples Federico II
Dept. Structures for Engineering and Architecture
P.le Tecchio 80
diana.faiella@unina.it

[3] University of Naples Federico II
Dept. Structures for Engineering and Architecture
P.le Tecchio 80
mario.argenziano@unina.it

Abstract

Mass damping is a well known principle for the reduction of structural vibrations and applied in tall building design in a variety of configurations. With mass usually small (around 1% of building mass), the properly "tuned" mass damper (TMD) shows great effectiveness in reducing wind vibrations, but minor advantages under earthquake excitations.
The above limitation can be surpassed by utilizing relatively large mass TMD. For this purpose, two different solutions are here proposed. In both cases, the idea is to separate the building into two or more parts, thus allowing for a relative motion between them, and activating the mass damping mechanism.
In the first solution, the building is subdivided along elevation into an upper and a lower structure, separated by means of an intermediate isolation system (IIS). In the second solution, by revisiting the classical mega-frame typology, the exterior full-height structure provides the global strength and stiffness, and secondary structures, extending between two transfer levels, are physically detached from the main structure at each floor and isolated at transfer level.
Simplified lumped-mass models are developed for illustrating the dynamic behaviour of the two solutions and carrying out parametric analyses. Procedures for deriving optimum values of design parameters are also proposed and compared to the parametric study.

Keywords: mass damping, motion based design, vibrations control, tall buildings, Mega Substructure Control System, Intermediate Isolation Systems.

1. INTRODUCTION

Mass Damping (MD) is nowadays a consolidate passive strategy, widely applied in tall building design since 1976 (John Hancock Tower in Boston) for mitigating structural vibrations and improve serviceability and occupant comfort [1]. A Tuned Mass Damper (TMD) is an auxiliary device attached to the main structure, consisting in a mass, spring, and damper. While TMDs with relatively small mass are very effective for reducing wind-induced response, they are not equally interesting under earthquake excitations [1 - 4].

In order to improve their seismic effectiveness, large mass TMDs can be utilized. With this choice, in fact, the system becomes most robust against deviations from design parameters and less dependent on the earthquake frequency content and the impulsive character of the seismic input [5]. This large mass can be obtained by converting a part of the structure into a huge mass damper, also appointed as non-conventional mass damper [5 - 9], thus combining control and structural functions. For this purpose, two different solutions are here proposed, by separating the building into two or more parts that vibrate out of phase and, thus, activate the mass damping mechanism.

In the first solution, the building is divided into two substructures, a lower and an upper structure, separated by means of a flexible horizontal disconnection, the isolation system, thus realizing an Intermediate Isolation System (IIS, Figure 1a). This configuration is widely utilized in Japan, where more than 60 buildings have been already realized [10], both for the seismic design of new buildings [11 - 17], and retrofit of existing buildings by means of vertical addition [13, 14]. While the IIS represents an extension of the Base Isolation System (BIS), its dynamics is more complicated due to the flexibility of the lower structure. In fact, the isolated upper structure behaves like a base isolated structure and as a large mass TMD for the lower structure [5 - 9, 18 - 26].

In the second solution, starting from the classical mega-frame typology for tall building structures [27 - 29], the building is subdivided in an exterior primary megastructure that provides the global strength and stiffness, and several interior secondary substructures, extending between two transfer levels, physically disconnected from the main structure at each floor and isolated at transfer level. Therefore, a Mega Substructure Control System (MSCS, Figure 1b) is realized, in which each isolated substructure behaves like a base isolated structure and the mass damping mechanism is activated by allowing the relative motion between the substructures and the main structure. This approach has been firstly proposed by Feng and Mita in 1995 [30], and then developed by the same authors [30 - 32] and by other researchers in a variety of solutions [34 - 45].

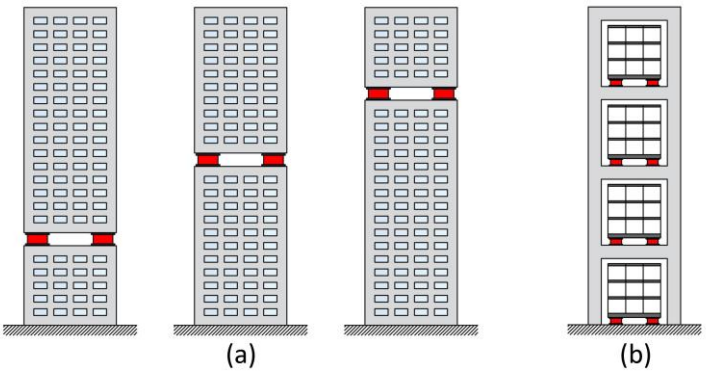

Figure 1: (a) Intermediate Isolation System (IIS) and (b) Mega-Substructure Control System (MSCS).

Both the mass damping solutions can be preliminary analysed by means of a simplified two-degree of freedom lumped mass model (2DOF MD, Figure 2b). For the Mega Substructure Control System, the main system accounts for the exterior megastructure, while the absorber globally represents the internal secondary substructures; instead, for the Intermediate Isolation System, the main and secondary system respectively refers to the lower structure and isolated upper structure. It is worth recalling that the IIS is generally analysed by means of a 3DOF model, accounting the DOFs

of the lower structure, the isolation system, and the upper structure. However, for evaluating its global dynamic behaviour, a 2DOF model can be adopted by satisfying the following two requirements: the upper structure is rigid with respect to the isolation system [46, 47], and the higher modes coupling is avoided [25, 48, 49].

In the present paper the dynamic behaviour of the two solutions is explored by carrying out parametric analyses on the simplified lumped mass model. The authors also propose procedures for deriving optimum values of the mass damper's design parameters, by minimizing the displacement amplitude of the main system under white noise. Finally, the optimal procedures are compared to the parametric study.

2. OPTIMIZATION PROCEDURE FOR NON-CONVENTIONAL MASS-DAMPING (MD) CONFIGURATIONS

Non-conventional mass-damping (MD) configurations utilising isolation system, such as Mega Substructure Control Systems and Intermediate Isolation Systems, can be preliminary analyzed by means of a simplified two degree-of-freedom (2DOF) lumped mass model, as depicted in Figure 2b. The first oscillator represents the main system with mass, stiffness, and damping coefficients named as m_1, k_1, and c_1, while the second oscillator represents the absorber (or secondary system) with mass, stiffness, and damping coefficients named as m_2, k_2, and c_2.

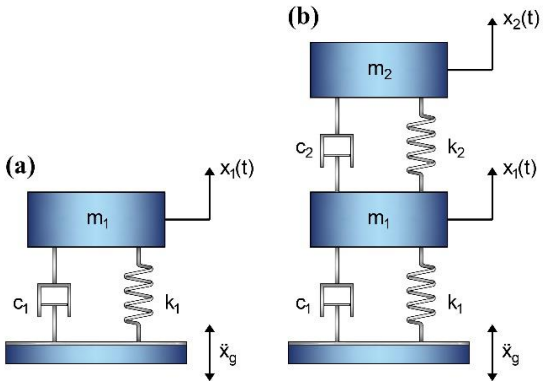

Figure 2: (a) simplified SDOF FB model, (b) simplified 2DOF MD model.

The equations of motion of the 2DOF MD model are:

$$\begin{cases} m_1\ddot{x}_1 + c_1\dot{x}_1 + k_1x_1 - c_2\left(\dot{x}_2 - \dot{x}_1\right) - k_2\left(x_2 - x_1\right) = -m_1\ddot{x}_g \\ m_2\ddot{x}_2 + c_2\left(\dot{x}_2 - \dot{x}_1\right) + k_2\left(x_2 - x_1\right) = -m_2\ddot{x}_g \end{cases} \tag{1}$$

being x_1 and x_2 the relative displacements of the two oscillators with respect to the ground and $\ddot{x}_g$ the ground acceleration.

By considering the stochastic nature of earthquake, the ground acceleration $\ddot{x}_g$ is modelled as a stationary Gaussian random process characterized by zero mean and white noise power spectral density $S_{\ddot{x}g}(\omega) = S_0$, in which there is no statistical correlation on what happens in two subsequent instants t_0 and $t_0+\tau$. Although it is neglected the dependency on the excitation frequency content, this process seems to be acceptable in an initial design phase, [e.g. 5].

For the 2DOF MD model shown in Figure 2, the optimization procedure provided by the authors is based on the minimization of the variance of the response x_1, $E[x_1^2]$ given by:

$$E\left[x_1^{\,2}\right] = S_0 \int_{-\infty}^{+\infty} \left|H_1(\omega)\right|^2 \partial\omega \tag{2}$$

where $H_1(\omega)$ is the transfer function of the displacement of the main system expressed in the frequency domain ω and obtained by means of the Fourier Transform of the linear differential equations (1) as a function of some dimensionless parameters:

$$H_1(\omega) = \frac{-i\omega^3 B_3 - \omega^2 B_2 + i\omega B_1 + B_0}{\omega^4 A_4 - i\omega^3 A_3 - \omega^2 A_2 + i\omega A_1 + A_0}, \tag{3}$$

where the coefficients $B_1 - B_3$ and $A_1 - A_4$ are:

$$B_0 = -\nu^2 \omega_1^2 (1+\mu);$$
$$B_1 = -2\xi_2 \nu (1+\mu)\omega_1 + 2\xi_1 \omega_1;$$
$$B_2 = -1;$$
$$B_3 = 0;$$

$$A_0 = \nu^2 \omega_1^4$$
$$A_1 = 2\xi_2 \nu \omega_1^3 + 2\xi_1 \nu^2 \omega_1^3$$
$$A_2 = \omega_1^2 + (1+\mu)\nu^2 \omega_1^2 + 4\xi_1 \xi_2 \nu \omega_1^2$$
$$A_3 = 2\xi_2 \nu \omega_1 (1+\mu) + 2\xi_1$$
$$A_4 = 1$$

and $\mu = m_2/m_1$ is the mass ratio, $\nu = \omega_2/\omega_1$ is the tuning ratio, ω_1 and ω_2 are the natural circular frequencies while $\xi_1 = c_1/(2m_1\omega_1)$ and $\xi_2 = c_2/(2m_2\omega_2)$ are the damping ratios of the main and secondary system, respectively.

The ranges of values selected for the non-dimensional parameters, covering a wide range of civil engineering applications, are: $\mu =]0, 2]$, $\nu =]0, 2]$, $\xi_1 = [0, 0.1]$, $\xi_2 = [0, 1]$.

By applying the Cauchy's residue theorem, the integral (2) can be analytically obtained [50, 51], leading to the following expression of $E[x_1^2]$:

$$E[x_1^2] = \frac{\pi S_0 \left(\frac{(A_2A_3 - A_1A_4)B_0^2}{A_0} + A_3\left(B_1^2 - 2B_0B_2\right) + \frac{(A_1A_2 - A_0A_3)B_3^2}{A_4} + A_1\left(B_2^2 - 2B_1B_3\right) \right)}{-A_0A_3^2 + A_1(A_2A_3 - A_1A_4)} \tag{4}$$

The square root of $E[x_1^2]$ is provided in Figure 3a and b, respectively for a damping ratio ξ_1 equal to 0 and 0.05. Each triplet of charts refers to mass ratios equal to 0.01, 0.1, and 1, by assuming unit values of the spectral density S_0 and the circular frequency ω_1. From Figure 3 it can be noticed that, by increasing the damping of the first oscillator for the same value of mass ratio, the variance of x_1 is reduced, highlighting the beneficial effect of ξ_1 in reducing the response of the main system. Instead, by increasing the mass ratio for the same value of ξ_1, the number of couples ξ_2-ν characterized by the same variance increases, leading to lower dependance of the response on the design parameters, and thus, to a major robustness of the system.

The minimization of the variance $E[x_1^2]$(4) is implemented by imposing that its gradient is null with respect to the tuning ratio ν and the damping ratio ξ_2, i.e.:

$$\begin{cases} \dfrac{\partial E\left[x_1^2\right]}{\partial \nu} = 0 \\ \dfrac{\partial E\left[x_1^2\right]}{\partial \xi_2} = 0 \end{cases} \tag{5}$$

The optimal values of the tuning ratio ν_{opt} and the damping ratio $\xi_{2,opt}$, obtained from Eq. (5), are presented in graphical form in Figure 4 by varying the damping ratio ξ_1 and considering the range of validity of the mass ratio μ equal to 0 – 1. In particular, the optimal tuning ratio decreases, and the optimal damping ratio increases, by increasing the mass ratio. From Figure 4 the effect of the first damping ratio on the trend of the optimal parameters can be also evaluated. While the distance between the optimal tuning curves becomes significant for ξ_1 equal to 0.05 and 0.1, with scatters up to 44% for medium-high mass ratios (Figure 4a), in terms of optimal damping curves, only for $\xi_1 = 0.1$ and for mass ratios approaching to 1, considerable scatters, up to 56%, are obtained (Figure 4b).

Depending on project specific considerations, related to both architectural/functional and constructive aspects, as well as to structural and dynamic requirements, the values of the optimal pa-

rameters cannot always be simultaneously adopted. In order to account these cases, starting from the optimizing conditions of Eq. (5), a single design variable is assumed, either the tuning ratio ν_{opt} or the damping ratio $\xi_{2,opt}$, while the other variable and the mass ratio are assumed as design data.

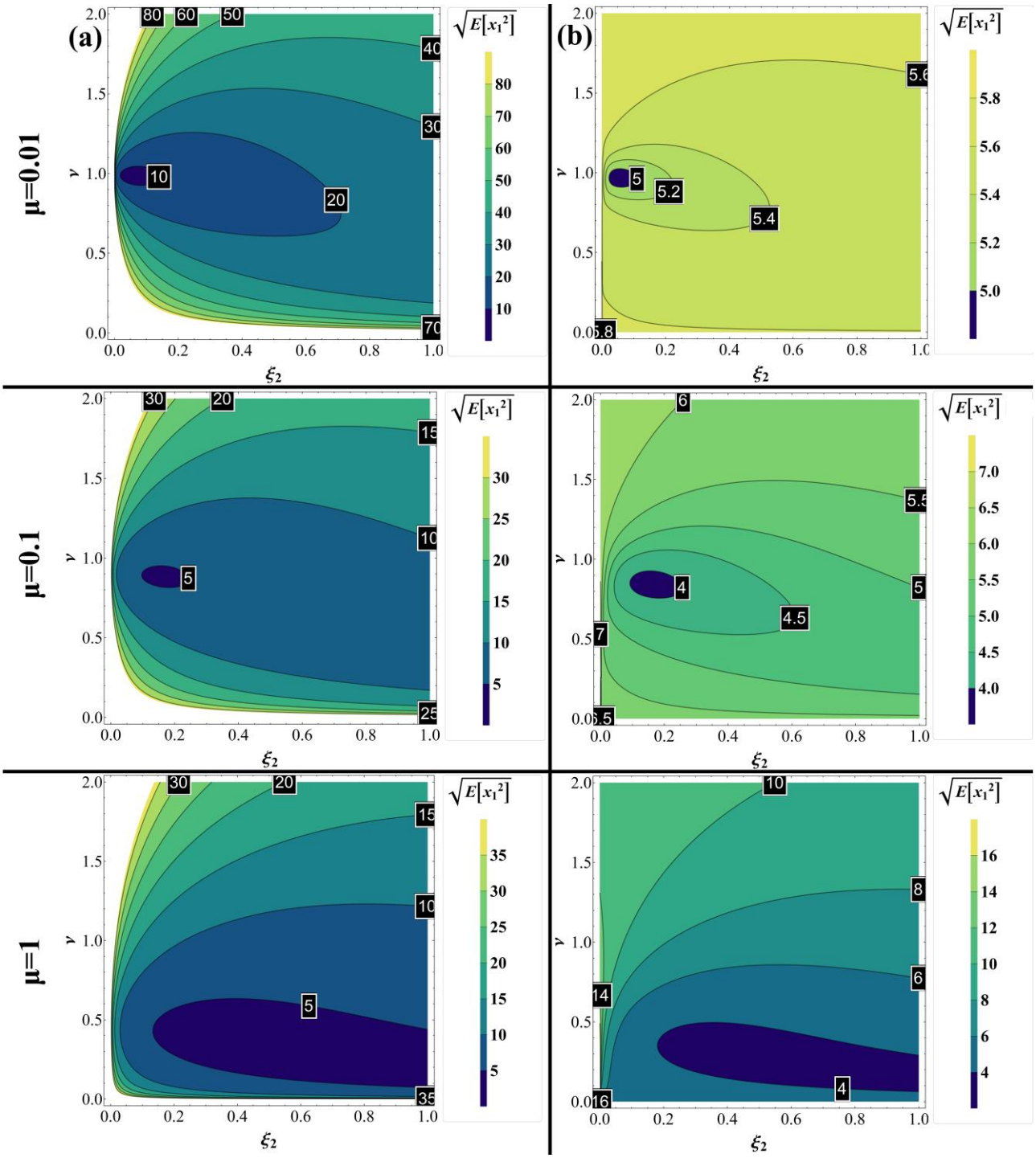

Figure 3: Response displacement of the main system: (a) first column $\xi_1 = 0$, (b) second column $\xi_1 = 0.05$.

Also for these optimization procedures, the values of the optimal parameters are provided in graphic form (Figure 5), by assuming the damping ratio ξ_1 equal to 0.05.

It is worth emphasizing that the first procedure proposed in this paper represents the generalization of the optimization algorithm implemented by [52]. In fact, by neglecting the damping of the main system, Warburton [52] imposes the minimization of the variance of the main system subjected to a white-noise input, with respect to ξ_2 and ν, thus analytically deriving optimal parameters.

Additionally, by considering a single design variable, ξ_2 or ν (Figure 5), the optimization method degenerates into the procedure proposed by [30], when the damping ratio of the main structure is assumed equal to 0 and ξ_2 is set equal to $(2m_2\omega_1)^{-1}$.

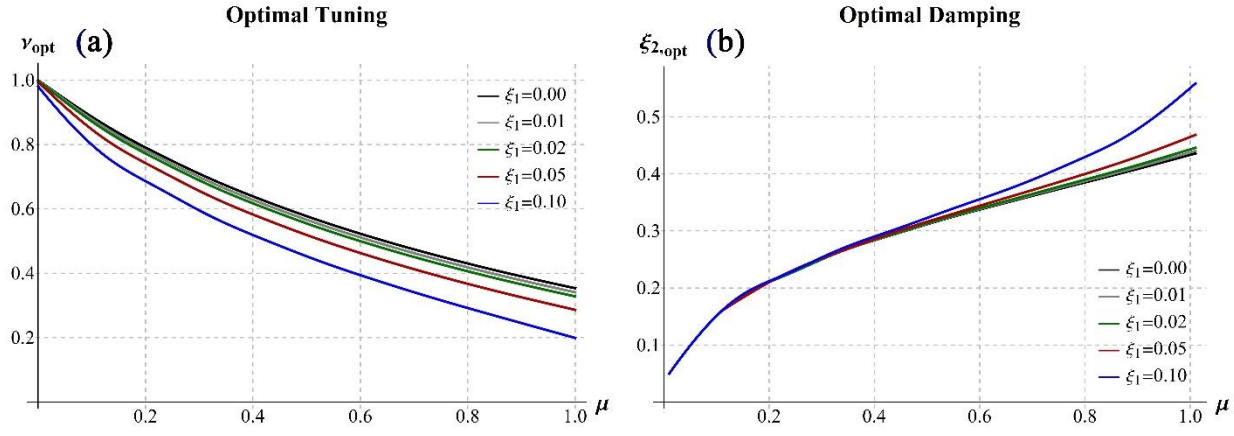

Figure 4: Optimal parameters: (a) tuning ratio ν_{opt}, (b) damping ratio $\xi_{2,opt}$.

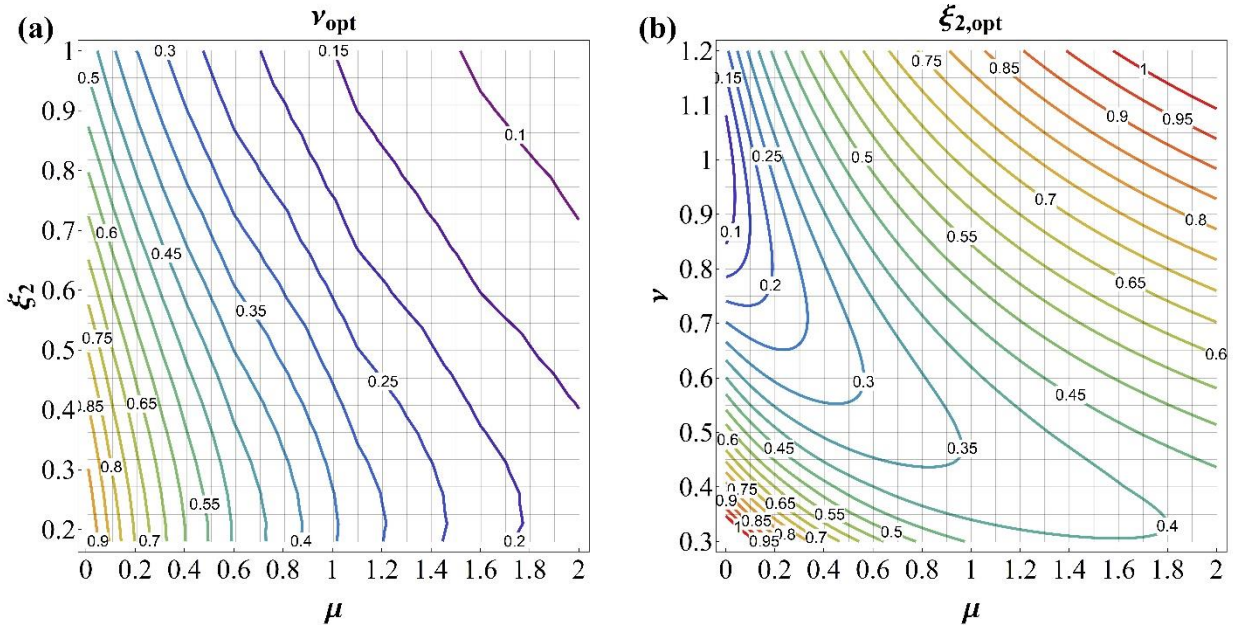

Figure 5: (a) optimal tuning ν_{opt} by varying ξ_2 and μ, (b) optimal damping $\xi_{2,opt}$ by varying ν and μ.

3. PARAMETRIC ANALYSIS

A wide parametric analysis is carried out for analysing the dynamic behaviour of non-conventional MD configurations and their potential benefits in reducing the seismic response of tall buildings, by adopting the simplified 2DOF model defined in the previous section 2 (Figure 2b). In particular, the dynamic characteristics of the MD models (periods and participating masses) are derived from classical modal analyses of the undamped system, while the complex eigenvalue problem has been solved in the state space for accounting the effect of the non-proportional damping. Then, response spectrum analyses are carried out by considering the complex modal superposition methods, in order to derive the base shear and displacement demands. Finally, time history analyses are performed for highlighting the effect of the seismic input (frequency content, duration, etc.), for discussing the effectiveness and robustness of the system, and for comparing different procedures of optimization.

3.1. Simplified models and design parameters

A 40-story tall building is adopted as a reference for the fixed-base (FB) single-degree of freedom model, by assuming the mass m_1 equal to 80000 kNs^2/m and the damping ratio ξ_1 equal to 0.05. Three baseline SDOF FB (Figure 2a) models are defined by varying the fundamental vibration period T_1, thus accounting for different structural solutions, from very rigid (*e.g. stiff diagrid structures or diagonalized mega-frame*) to more flexible structural systems (*e.g. moment resisting frames or frame tubes*). In particular, the fundamental vibration periods T_1 are assumed equal to 1.62 s, 2.5 s, 3.5 s.

The design parameters adopted for exploring the dynamic behaviour of the controlled 2DOF MD configurations (Figure 2b) are the mass ratio μ, the isolation period T_2, and the damping ratio of the isolation system ξ_2, which vary in the following ranges:

- T_2 = 0.05 – 10 s (50 values);
- μ = 0.1, 0.5, 1.0, 1.5;
- ξ_2 = 0.05 – 0.5 (26 values).

Hence, by varying all the design parameters, a total of 15600 models have been generated.

It is worth observing that, while some values of the mass ratios and of the isolation periods are not realistic, they are considered herein to fully characterize the behaviour of the system and provide a comprehensive view of its potential applications and limitations. The range for the damping ratio ξ_2 has been chosen considering different isolation systems, composed either by high damping rubber bearings or by natural rubber bearings plus viscous or hysteretic dampers.

3.2. Non-proportional damping and complex mode superposition method

In the controlled MD configurations, the structural damping ξ_1 is assumed equal to 0.05 while the damping of the isolation system ξ_2 varies between 0.05 and 0.50. Structures with very different values of damping ratios represent non-proportional (or non-classical) damped system, characterized by complex-valued natural modes. In this case, the off-diagonal terms in the damping matrix **C** cannot be neglected, since the system does not satisfy the Caughey and O' Kelly identity: $\boldsymbol{CM}^{-1}\boldsymbol{K} = \boldsymbol{KM}^{-1}\boldsymbol{C}$ (with $\boldsymbol{M}$, $\boldsymbol{K}$, and $\boldsymbol{C}$ the mass, stiffness and damping matrices) [53]. Furthermore, when $\boldsymbol{C}$ is an arbitrary symmetric positive-definite matrix, the expansion in terms of the eigenvectors for the undamped system and real modal coordinates does not lead to uncoupled modal equations. Therefore, rather than working with a second-order equation, it is more convenient to transform the equations of motion into a set of first-order equations involving complex modal coordinates and complex state eigenvectors, and working in the state space [54].

In the response spectrum analyses carried out in the following section, the complete-quadratic-combination (CQC) rule is utilized in order to obtain the maximum responses associated to each degree of freedom. Being the system non-classically damped, the method described by Sinha and Igusa [55] is utilized in order to consider the complex-valued nature of the vibration mode shapes. Therefore, the maximum system response, R, is given by:

$$R = \sqrt{\sum_{i=1}^{n}\sum_{j=1}^{n} B_i B_j \rho_{ij} R_i R_j} \tag{6}$$

with n the number of the considered vibration mode; B_i and B_j real-valued participation factors; R_i and R_j spectral displacements; ρ_{ij} real-valued modal correlation factors. The participation factors and modal correlation factors depend on the vector that defines which DOF is being considered; therefore, they assume different values when evaluating the response of each floor, differently to what is done in the case of CQC rule for classically damped systems, where these parameters are fixed quantities [56].

3.3. Response spectrum analysis (RSA)

Response spectrum analyses (RSA) are carried out on all the simplified MD and FB models by utilizing the acceleration response spectrum defined by the Eurocode 8 [57] for the design earthquake, characterised by 10 % probability of exceedance in 50 years (475 years Return Period).

The spectrum is depicted in Figure 6a, for a_g = 0.35 g, soil type B (S = 1.2; T_B = 0.15 s; T_C = 0.5 s; T_D = 2 s), damping ratio equal to 0.05. The complex mode superposition method proposed by Sinha and Igusa [55], briefly recalled in section 3.2, has been used to consider the complex-valued nature of the vibration mode shapes. In Figures 6b and 7 the results of the analyses are firstly presented for the case of ξ_2 = 0.30; then the effect of the damping ratio of the isolation system is evaluated in Figure 8.

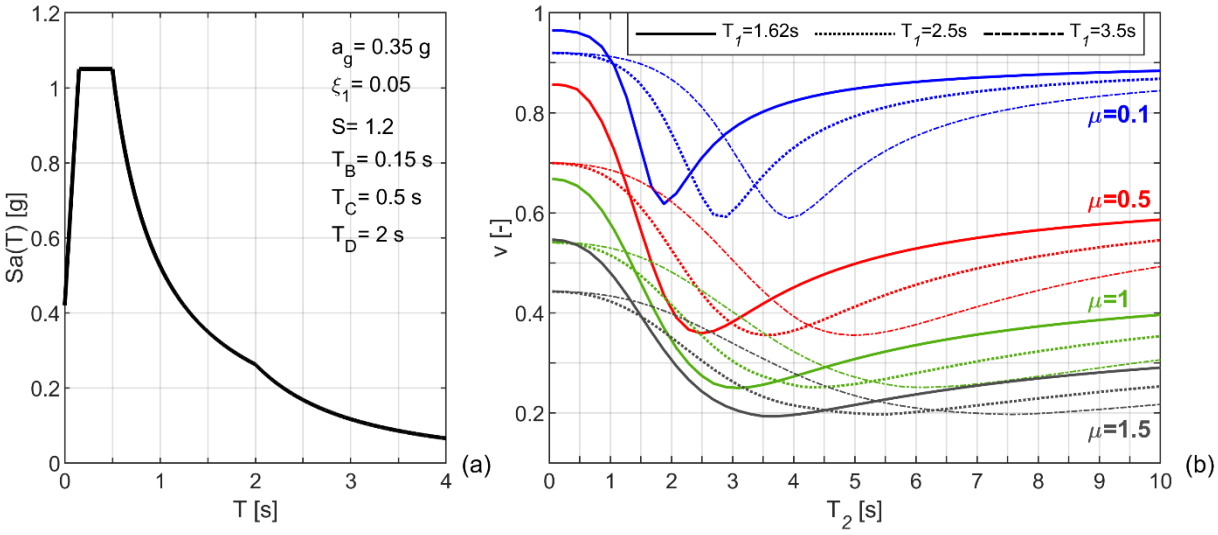

Figure 6: (a) EC8 elastic acceleration response spectrum, (b) base shear ratio v vs. T_{ISO}. for ξ_2 = 0.30.

The Figure 6b depicts the base shear ratio between the base shear controlled MD configuration and the uncontrolled FB counterpart, i.e. $v=V_{MD}/V_{FB}$, as a function of the isolation period T_2. From the chart, it can be immediately observed that the base shear ratio v is always less than one, approximately between 0.95 e 0.85 for μ=0.1, between 0.85 e 0.50 for μ =0.5, between 0.68 e 0.30 for μ =1, between 0.55 e 0.20 for μ =1.5, showing significant reduction by increasing the mass ratio.
Considering the trend of v for each mass ratio, three behavioural zone can be clearly identified. The *first zone* (e.g. very small values of T_2) corresponds to the largest values of v, since the two parts are rigidly connected, thus no relative motion is allowed and no mass-damping mechanism arises. In particular, the first mode is the mode of the main structure, which activates all the mass of the system and, due to the presence of the secondary system, shows a period slightly elongated with respect to the uncontrolled baseline counterpart. Therefore, the base shear assumes values slightly lower than the FB counterpart and the ratio becomes less than one. The *second zone* (e.g. very large values of T_2) shows base shear ratios that reach the relevant mass fractions of the primary system $m_1/(m_1+m_2)$. In particular, the dynamic behaviour of the system tends to a condition of "perfect isolation", with the masses of the two systems almost completely decoupled, and the first and second mode respectively corresponding to the mode of the secondary and main system. The *third zone* (e.g. intermediate values of T_2) presents the minimum values of v, thanks to maximum exploitation of the mass damping mechanism. In this zone, the first and second modes are still the modes of the secondary and primary system. However, the interaction between the two parts leads to a transfer of a fraction of the main system's mass from the second to the first mode, with a consequent significant reduction of the ratio v.

In Figure 7 the shear ratio charts (v- T_2) for three values of T_1 (1.62, 2.5, 3.5 s) are coupled to the analogous charts depicting the displacement of the primary system in the MD configuration normalized to the FB counterpart, i.e. $d = d_{1,MD}/d_{1,FB}$, and the deformation in the isolation system δ_2, as a

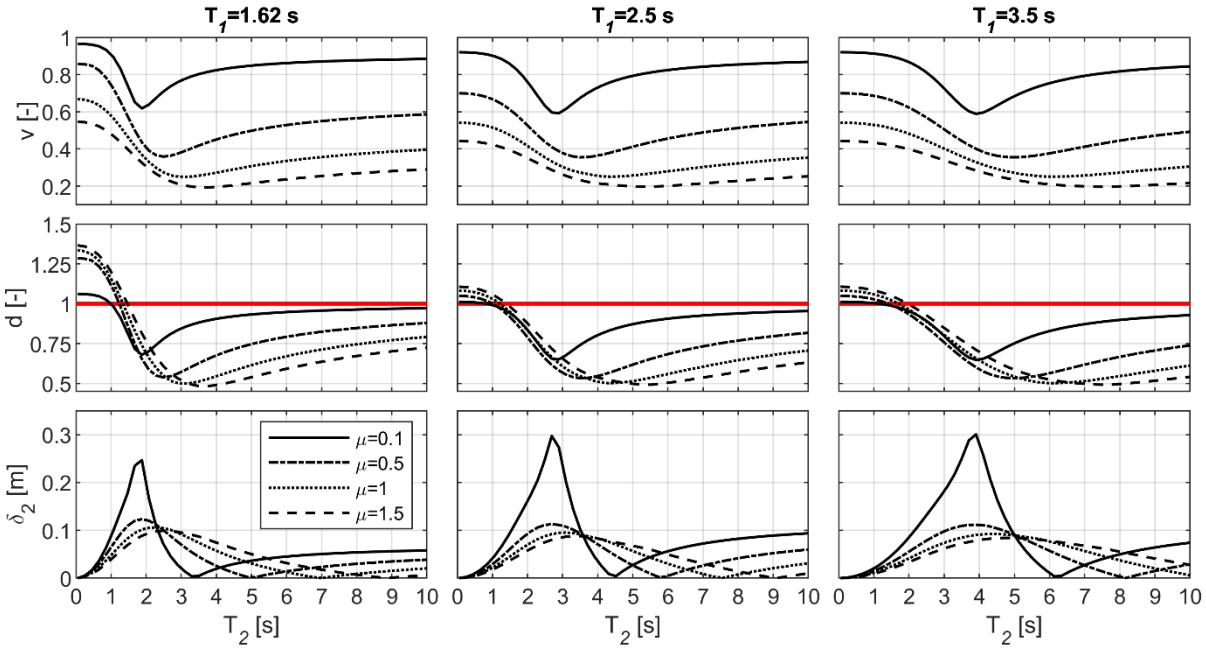

(a) (b) (c)

Figure 7: Ratios v, d, and relative displacement δ_2 for ξ_2 = 0.30: (a) T_1 = 1.62 s, (b) T_1 = 2.5 s, (c) T_1 = 3.5 s.

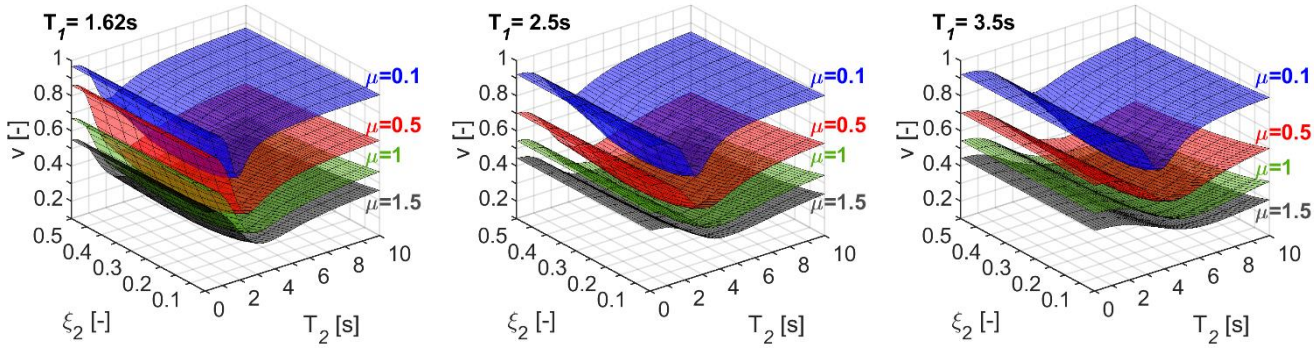

(a) (b) (c)

Figure 8: Base shear ratio v as a function of ξ_2 and T_2 for (a) T_1 = 1.62 s, (b) T_1 = 2.5 s, (c) T_1 = 3.5 s.

function of T_2. Quite trivially, it can be observed that the minimum values of v and d are obtained for the same value of T_2, which also corresponds to the maximum deformation in the isolation system.

For the three baseline models, Figure 8 provides the trend of the shear ratio v as a function of the isolation period T_2 and the damping ratio ξ_2, for each value of the mass ratio μ. It can be observed that, in the third zone of "perfect isolation", the shear ratio v is reduced by increasing T_1, therefore the effect of ξ_2 becomes more significant for more flexible baseline models and isolation systems. In the second zone in which the mass damping mechanism is maximized and the primary and secondary systems are strongly coupled, the minimum values of v are obtained for values of ξ_2 between 0.2 – 0.4, as discussed in detail in the following section.

3.4. Comparison between the results of optimal procedures and of the parametric analysis

In this section the optimal values of the parameters ν e ξ_2 derived from the results of the RSA are compared to the ones calculated by means of the optimal procedures provided in section 2. For the sake of brevity, only the results obtained for the MD controlled configuration characterized by T_1 = 1.62 s and μ = 1 are presented in the following.

In particular, six optimal configurations are defined and named as A, B, C, D, FM, W. The solution A represents the optimal configuration that gives rise to the minimum values of the base shear, and of the displacement of the primary system, obtained through the RSA. The solutions B and C are derived by assuming respectively ξ_{2opt} or ν_{opt} from the optimal procedures of section 2, while the other one is retrieved from the parametric analysis (Figure 5); the solution D is entirely derived through the optimization procedure, i.e. the optimal values of both parameters are simultaneously considered (Figure 4). The solutions FM and W are derived by adopting the optimal parameters of the procedures suggested by Feng and Mita [30] and Warburton [52], respectively. The values of the optimal parameters, of the corresponding two complex modal damping ratios η_1 and η_2, as well as of the shear ratio v, of the six solutions are reported in Table 1. It can be observed that, the solutions A and B provide the minimum shear ratio v, equal to 0.25, while the other solutions show values of the shear ratio varying between 0.28 and 0.34.

Ref.		Optimal Solutions	ν_{opt} -	ξ_{2opt} -	T_{2opt} s	η_1 -	η_2 -	v -
This paper	RSA	A	0.523	0.33	3.10	0.207	0.267	0.25
	RSA+OPT	B	0.523	0.36	3.10	0.225	0.289	0.25
	OPT+RSA	C	0.330	0.33	4.91	0.281	0.172	0.30
	OPT	D	0.325	0.47	4.98	0.409	0.220	0.29
Feng and Mita		FM	0.353	0.15	4.59	0.124	0.108	0.34
Warburton		W	0.353	0.43	4.59	0.365	0.225	0.28

Table 1: Dynamic properties of the six optimal solutions.

3.5. Time history analyses

In order to assess and compare the response of the six controlled configurations under real seismic inputs, time history analyses are carried out on the relevant MD and FB models. A set of ten records registered during real earthquakes is used and scaled by means of the software SeismoMatch [58], by checking the closeness of their average response spectrum to the target elastic spectrum (provided in Figure 6a) in the period range 0.05 - 4 s. Data of the ten scaled ground motions and corresponding acceleration response spectra, with the average spectrum, are given in Figure 9.

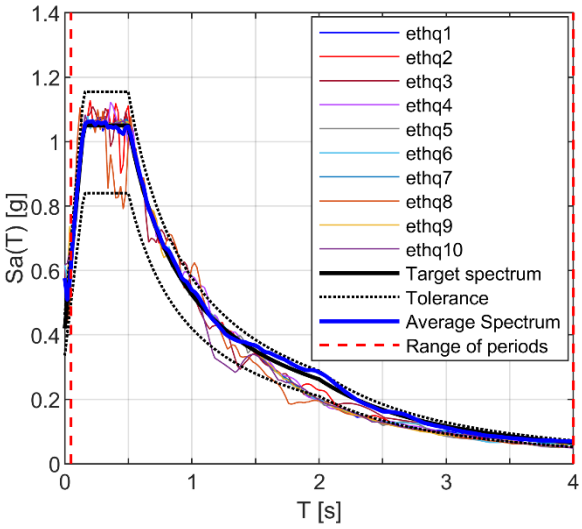

Earthquake name		Date	Comp.	PGA [g]
ethq1	Imperial Valley	18/05/1940	S00E	0.425
ethq2	Taft	21/07/1952	S69E	0.482
ethq3	Hachinohe	16/05/1968	NS	0.490
ethq4	Loma Prieta	17/10/1989	NS	0.511
ethq5	Northridge	17/01/1994	S90W	0.547
ethq6	Kobe	17/01/1995	000	0.571
ethq7	L'Aquila	04/04/2009	EW	0.472
ethq8	Chile	27/02/2010	NS	0.437
ethq9	Christchurch	22/02/2011	N55W	0.551
ethq10	Amatrice	24/08/2016	EW	0.617

Figure 9: Major data and acceleration response spectra of the scaled acceleration records.

The results of the analyses are here provided in Figures 10 and 11 in terms of base shear, relative displacements, floor absolute accelerations, by comparing the six controlled configurations and each MD configuration to the FB counterpart.

The Figure 10 depicts for each optimal solution the average peak response registered during the ten acceleration histories in terms of some response parameters. These parameters express the response of the controlled configuration normalized to the uncontrolled counterpart, considering the base shear, v, the relative displacement, d, and absolute acceleration, a, of the primary structure. The remarkable effectiveness of the controlled configurations emerges in terms of all the response parameters. In fact, the shear ratio v varies between 0.194 and 0.345, the displacement ratio d between 0.388 and 0.689, and the acceleration ratio a between 0.553 and 0.726. In particular, the solution B provides the maximum reductions, with values very close to the ones of the solution A, while the solution FM shows the minimum reductions and thus it represents the less efficient solution.
The average envelopes of the peak displacements and absolute accelerations, obtained from the time history analyses of the controlled configurations and baseline structure, are shown in Figure 11. From the graphs it can be observed that, for all the optimal solutions the average values of story drift and absolute acceleration in the MD models are reduced with respect to the FB uncontrolled structure. The solutions A and B are confirmed the most effective in reducing the seismic response of the primary system.

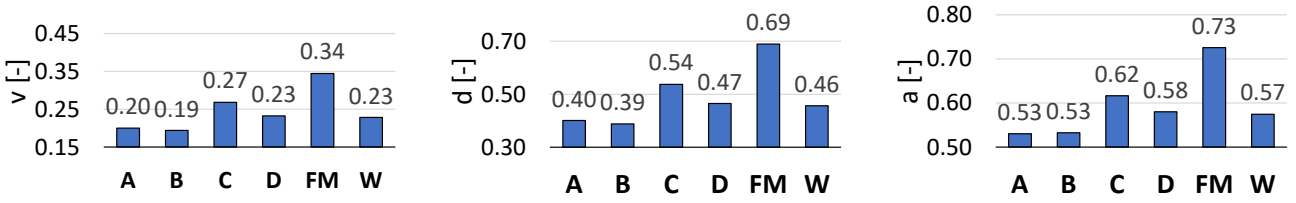

(a) (b) (c)

Figure 10. Comparison between the six optimal solutions: (a) base shear ratio v, (b) displacement ratio d, (c) acceleration ratio a.

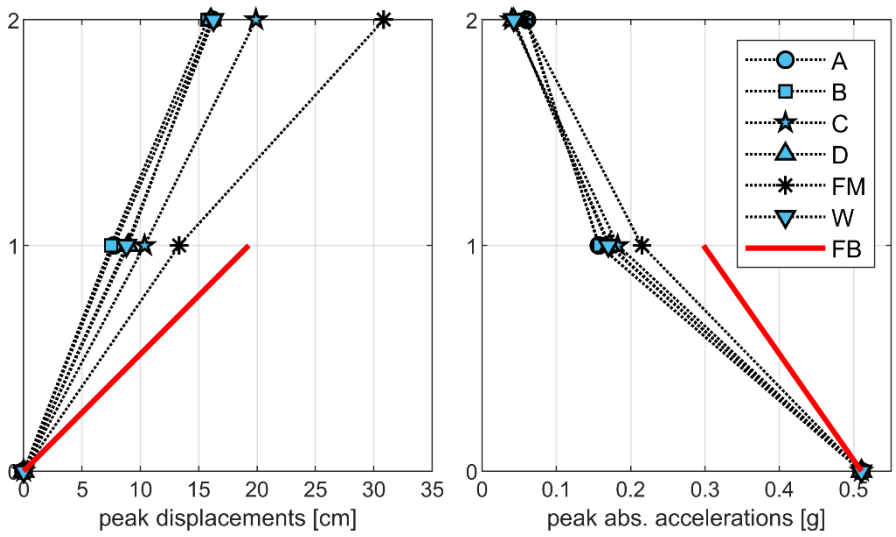

Figure 11: Peak story displacements and absolute accelerations for the six optimal solutions.

4. SUMMARY AND CONCLUSIONS

In the present paper, the authors investigate the dynamic behaviour of mass damping (MD) configurations utilising isolation system, such as Mega Substructure Control Systems and Intermediate Isolation Systems, by preliminary adopting simplified lumped mass 2-DOF models. By considering a stochastic approach, the seismic acceleration is modelled as a white noise and the variance of the displacement of the first degree of freedom is minimized in the first instance with respect to both design variables, i.e. the tuning ratio and the damping ratio of the secondary system and secondly with respect to only one of these two variables. Furthermore, in order to validate this general proce-

dure, a wide parametric analysis is carried out on simplified lumped mass models and the potential benefits of such systems in reducing the seismic response of tall buildings is examined.

In particular, by selecting a 40-story tall building and by varying the mass ratio, classical and complex modal analyses show three different dynamic behavioural zones as a function of the isolation period: the first zone is characterized by a "fixed-base" behaviour, in the second zone the interaction between the two masses gives rise to the mass damping effect, while in the third zone for very long isolation periods, the two structural parts are almost dynamically decoupled.

Then, response spectrum analyses with complex modal superposition methods are performed, with the aim to compare the base shear and the displacement demands with the fixed-base counterpart simplified SDOF model. More in detail, a significant reduction of the seismic demand on the main system is observed when large mass ratios are adopted for the whole range of the isolation period, thus confirming the structural robustness of such systems. Finally, time history analyses are implemented for underlining the effects of the seismic input (amplitude, frequency content, duration, etc.) and for comparing the results of different procedures of optimization, both those proposed in the present work and those of existing literature.

References

[1] Holmes D., Listing of installations, Engineering Structures 1995, 17(9):676–678.
[2] Kaynia A.M., Veneziano D., Seismic effectiveness of tuned mass dampers, Journal of the Structural Division 1981, ASCE, 107(8):1465–1484.
[3] Sladek J.R., Klingner R.E., Effect of tuned mass dampers on seismic response. Journal of Structural Engineering 1983, ASCE; 109(8):2004–2009.
[4] Soto-Brito R., Ruiz S.E., Influence of ground motion intensity on the effectiveness of tuned mass dampers, Earthquake Engineering and Structural Dynamics 1999, 28(11):1255–1271.
[5] De Angelis M., Perno S., Reggio A. 'Dynamic response and optimal design of structures with large mass ratio TMD'. *Earthquake Engng Struct. Dyn*. 2012, vol. 41(1), pp. 41–60. https
[6] Reggio A. and De Angelis M. 'Optimization of a Non-Conventional TMD implemented via Inter-story Isolation'. *Proceedings of the EURODYN 2014 – IX International Conference of Structural Dynamics*; Porto, Portugal, 30 June – 2 July 2014. pp. 1713–1720
[7] Reggio A. and De Angelis M. 'Optimal energy-based seismic design of non-conventional tuned mass damper (TMD) implemented via inter-story isolation'. *Earthquake Eng Struct. Dyn*. 2015, vol. 44(10), pp. 1623–1642. https ://doi.org/10.1002/eqe.2548
[8] Wang S.J., Lee B.H., Chuang W.C., Chang K.C. 'Optimum dynamic characteristic control approach for building mass damper design'. *Earthquake Engng Struct Dyn*. 2018, vol. 47(4), pp. 872–888. https ://doi.org/10.1002/eqe.2995
[9] Wang S.J., Lee B.H., Chuang W.C., Chiu I.C., Chang K.C. 'Building mass damper design based on optimum dynamic response control approach'. *Eng Struct*. 2019; vol. 187, pp. 85–100. https ://doi.org/10.1016/j.engst ruct.2019.02.053
[10] Kobayashi M. and Sasaki D. 'Making a seismic design database of mid-story isolated buildings and structural property evaluation based on response prediction method'. *AIJ J Technol Des*, Feb 2009, vol. 15(29), pp. 65–70. https ://doi.org/10.3130/aijt.15.65 (in Japanese)
[11] Murakami K., Kitamura H., Ozaki H., Teramoto T. 'Design and analysis of a building with the middle-story isolation structural system'. *Proceeding of the 12th World Conference on Earthquake Engineering*; Auckland, New Zealand, 30 Jan – 4 Feb 2000, paper 0857
[12] Sueoka T., Torii S., Tsuneki Y. 'The application of response control design using middle-story isolation system to high-rise building'. *Proceeding of the 13th World Conference on Earthquake Engineering*; Vancouver, B.C., Canada, Aug 2004, paper 3457
[13] Tsuneki Y., Torii S., Murakami K., Sueoka T. 'Middle-story Isolated Structural System of High-Rise Building'. *Proceedings of the 14th World Conference on Earthquake Engineering*; Beijing, China, Oct 2008, paper S05-01-023.f

[14] Tsuneki Y., Torii S., Murakami K., Sueoka T. 'Middle-story isolated structural system of high-rise building'. *J Disaster Res*. 2009, vol. 4(3), pp. 229–238. https ://doi.org/10.20965 /jdr.2009.p0229
[15] Okada K., Yoshida S. 'Structural design of Nakanoshima festival tower'. *Int J High-Rise Build*. 2014, vol. 3(3), pp. 173–183
[16] Nakagawa K., Shimazaki D., Yoshida S., Okada K. 'Application of Seismic Isolation Systems in Japanese high-rise buildings'. *International Journal of High-Rise Buildings*. 2015. Seismic Design Issue II. pp. 36-38.
[17] Tamari M., Yoshihara T., Miyashita M., Ariyama N., Nonoyama M. 'Structural Design and Performance Evaluation of a Mid-story Seismic Isolated High-Rise Building'. International Journal of High-Rise Buildings. 2017. Vol. 6(3), pp. 227-235. https://doi.org/10.21022/IJHRB.2017.6.3.227
[18] Villaverde R. 'Reduction seismic response with heavily-damped vibration absorbers'. *Earthquake Eng Struct Dyn*. 1985, vol. 13(3), pp. 33–42. https ://doi.org/10.1002/eqe.42901 30105
[19] Sadek F., Mohraz B., Taylor A.W., Chung R.M. 'A method of estimating the parameters of tuned mass dampers for seismic applications'. *Earthquake Engng Struct Dyn*. 1997, vol. 26(6), pp. 617–635. https ://doi.org/10.1002/(SICI)1096-9845(19970 6)26:6%3c617 :AID-EQE66 4%3e3.0.CO;2-Z
[20] Tan P., Zhang Y, Zhou F. 'Optimal Design and Control Mechanism Study on Story Isolation System'. *Proceedings of the 14th World Conference on Earthquake Engineering*; Beijing, China, Oct 2008, paper 0060.
[21] Chey M., Chase J.G., Mander J.B., Carr A.J. 'Innovative seismic retrofitting strategy of added stories isolation system'. *Front Struct Civ Eng*. 2013, vol. 7(1), pp. 13–23. https ://doi.org/10.1007/s1170 9-013-0195-9
[22] Miranda J.C. 'A method for tuning tuned mass dampers for seismic applications'. *Earthquake Engng Struct Dyn*. 2013, vol. 42(7), pp. 1103-1110. https://doi.org/10.1002/eqe.2271
[23] Zhou Q, Singh MP, Huang XY (2016) Model reduction of mid-story isolation systems. Eng Struct 124:36–48. https ://doi.org/10.1016/j.engst ruct.2016.06.011
[24] Argenziano M., Faiella D., Fraldi M., Mele E. 'Optimum tuning frequency and damping ratios in Inter-story Isolation Systems (IIS): a closed form solution'. *XVIII Convegno Anidis*; Ascoli Piceno, Italy, Sept 2019.
[25] Faiella D., Mele E. 'Vibration Characteristics and Higher Mode Coupling in Intermediate Isolation Systems (IIS). A Parametric Analysis'. *Bull Earthq Eng*. 2019, vol. 17(7), pp. 4347–87. https://doi.org/10.1007/s10518-019-00637-w.
[26] Faiella D., Mele E. 'Insights into inter-story isolation design through the analysis of two case studies'. *Eng Struct*. 2020, vol. 215, pp. 1-21. https://doi.org/10.1016/j.engstruct.2020.110660
[27] Goldsmith M. 'The tall buildings: the effect of scale'. Master's thesis, Illinois Institute of Thecnology, Chicago, Illinois, 1953.
[28] Ali M.M. (2001). Art of the skyscraper. The genius of Fazlur Khan. Rizzoli International Publications Inc, New York.
[29] Khan Y.S. (2004). Engineering Architecture. The vision of Fazlur R. Khan. W W Norton & Co Inc, New York.
[30] Feng M.Q, Mita A. (1995). Vibration control of tall buildings using mega subconfiguration, Journal of Engineering Mechanics, 121(10):1082-1088.
[31] Chai W., Feng M.Q.. (1996). Seismic performance of mega-sub controlled buildings. The 11th World Conference on Earthquake Engineering, June 23-28, 1996, Acapulco, Mexico. Paper no. 789.
[32] Chai W., Feng M.Q.. (1997). Vibration control of super tall buildings subjected to wind loads. International Journal of Non-Linear Mechanics, 32(4): 657-668. https://doi.org/10.1016/S0020-7462(96)00094-7

[33] Feng M.Q., Chai W.. (1997). Design of mega-sub controlled building system under stochastic wind loads. Probabilistic Engineering Mechanics, 12(3): 149-162. https://doi.org/10.1016/S0266-8920(96)00035-5
[34] Zhang X.A, Wang D., Jiang J. (2005) The controlling mechanism and the controlling effectiveness of passive mega-sub-controlled frame subjected to random wind loads. Journal of Sound and Vibration 283(3-5), 543–560. https://doi.org/10.1016/j.jsv.2004.04.038
[35] Zhang X.A., Zhang J., Wang D., Jiang J. (2005) Controlling Characteristics of Passive Mega-Subcontrolled Frame Subjected to Random Wind Loads. Journal of Engineering Mechanics, 131(10):1046-1055.
[36] Zhang X.A, Qin X., Cherry S., Lian Y., Zhang J., Jiang J. (2009) A New Proposed Passive Mega-Sub Controlled Structure and Response Control, Journal of Earthquake Engineering, 13:2, 252-274. https://doi.org/10.1080/13632460802347422
[37] Kalehsar H.E, Khodaie N. (2018) Wind-induced vibration control of super-tall buildings using a new combined structural system. Journal of Wind Engineering & Industrial Aerodynamics, 172, 256–266.
[38] Li T., Zhang X.A, Wang Q. (2011) Control Characteristics of Mega-sub Controlled Structure System with Friction Damper under Rare Earthquake. Proceedings of the International MultiConference of Engineers and Computer Scientists 2011 Vol II; Hong Kong, China, Mar 2011. pp. 791 – 796.
[39] Li X., Tan P., Li X., Liu A. (2016) Mechanism Analysis and Parameter Optimization of Mega-Sub-Isolation System. Shock and Vibration. Vol. 2016, pp. 1-12. Article ID 2605839. https://doi.org/10.1155/2016/2605839
[40] Tan P., Zhang Y., Li X., Li X., Liu A., Zhou F. (2016) Experimental investigation of mega-sub isolation structure'. Struct Design Tall Spec Build, vol. 26(16), e1360. https://doi.org/10.1002/tal.1360
[41] Ye Z. and Wu G. (2017) Optimal lateral aseismic performance analysis of mega-substructure system with modularized secondary structures. Struct Design Tall Spec Build., vol. 26, e1387. pp. 1-14. https://doi.org/10.1002/tal.1387
[42] Huang J.Q, Chong X. Jiang Q., Ye X.G, Wang H.Q. (2018) Seismic Response Reduction of Megaframe with Vibration Control Substructure. Shock and Vibration Volume 2018, Article ID 9427908.
[43] Martinez-Paneda M, Elghazouli A.Y (2020) An integrated damping system for tall buildings. The Structural Design of Tall and Special Buildings, vol. 29(7), e1724. https://doi.org/10.1002/tal.1724
[44] Kawai A., T. Maeda, Takewaki I. (2020) Smart Seismic Control System for High-Rise Buildings Using Large-Stroke Viscous Dampers Through Connection to Strong-Back Core Frame. Front. Built Environ., vol. 6(29), pp. 6-29. https://doi.org/10.3389/fbuil.2020.00029
[45] Liang Q., Li L., Yang Q. (2020) Seismic analysis of the tuned-inerter-damper enhanced mega-sub structure system'. Struct Control Health Monit., e2658. pp. 1-15. https://doi.org/10.1002/stc.2658
[46] Kelly J (1997) Earthquake resistant design with rubber. Springer, Berlin
[47] Naeim F, Kelly J (1999) Design of seismic isolated structures: from theory to practice. Wiley, Hoboken
Wang et al., 2012
[48] Wang SJ, Chang KC, Hwang JS, Hsiao JY, Lee BH, Hung YC (2012) Dynamic behaviour of a building structure tested with base and mid-story isolation systems. Eng Struct 42:420–433. https ://doi.org/10.1016/j.engst ruct.2012.04.035
[49] Kobayashi M, Koh T (2008) Modal coupling effects of mid-story isolated buildings. In: 14th World conference on earthquake engineering, Beijing, China, paper 05-01-0230
[50] James, H. M., Nichols, N. B., & Phillips, R. S. (Eds.). (1947). *Theory of servomechanisms* (Vol. 25). New York:

[51] Crandall, S. H., & Mark, W. D. (2014). *Random vibration in mechanical systems*. Academic Press.
[52] Warburton G.B., Optimum absorber parameters for various combinations of response and excitation parameters, Earthquake Engineering and Structural Dynamics 1982, 10(3):381-401.
[53] Veletsos A.S., Ventura C.E. 'Modal Analysis of non-classically damped linear systems', *Earthquake Engng Struct Dyn.* 1986, vol. 14(2), pp. 217–243.
https://doi.org/10.1002/eqe.4290140205
[54] Connor J., Laflamme S. *Structural Motion Engineering*. Berlin: Springer; 2014.
[55] Sinha R. and Igusa T. 'CQC and SRSS methods for non-classically damped structures'. *Earthquake Engng Struct Dyn*. 2012, vol. 24(4), pp. 615-619. https://doi.org/10.1002/eqe.4290240410
[56] Moutinho C. 'An alternative methodology for designing tuned mass dampers to reduce seismic vibrations in building structures'. *Earthquake Engng Struct Dyn*. 2012, vol. 41(14), pp. 2059-2073. https://doi.org/10.1002/eqe.2174
[57] Code, P. (2005). Eurocode 8: Design of structures for earthquake resistance-part 1: general rules, seismic actions and rules for buildings. *Brussels: European Committee for Standardization*.
[58] SeismoMatch, SEiSMOSOFT, Earthquake Engineering Software Solutions.